Reliability Engineering and System Safety 137 (2015) 40–49

Contents lists available at ScienceDirect

Reliability Engineering and System Safety

journal homepage: www.elsevier.com/locate/ress

First and second order approximate reliability analysis methods using evidence theory

Z. Zhang [a], C. Jiang [a,*], G.G. Wang [b], X. Han [a]

[a] State Key Laboratory of Advanced Design and Manufacturing for Vehicle Body, College of Mechanical and Vehicle Engineering, Hunan University, Changsha City 410082, PR China

[b] Product Design and Optimization Lab, School of Mechatronic Systems Engineering, Simon Fraser University, Surrey, BC, Canada V3T 0A3

ARTICLE INFO

Article history:
Received 5 May 2014
Received in revised form
23 December 2014
Accepted 25 December 2014
Available online 1 January 2015

Keywords:
Structural reliability
Evidence theory
Epistemic uncertainty
Reliability interval
First order approximation
Second order approximation

ABSTRACT

The first order approximate reliability method (FARM) and second order approximate reliability method (SARM) are formulated based on evidence theory in this paper. The proposed methods can significantly improve the computational efficiency for evidence-theory-based reliability analysis, while generally provide sufficient precision. First, the most probable focal element (MPFE), an important concept as the most probable point (MPP) in probability-theory-based reliability analysis, is searched using a uniformity approach. Subsequently, FARM approximates the limit-state function around the MPFE using the linear Taylor series, while SARM approximates it using the quadratic Taylor series. With the first and second order approximations, the reliability interval composed of the belief measure and the plausibility measure is efficiently obtained for FARM and SARM, respectively. Two simple problems with explicit expressions and one engineering application of vehicle frontal impact are presented to demonstrate the effectiveness of the proposed methods.

1. Introduction

Uncertainties widely exist in practical engineering problems, which should be appropriately quantified and controlled for the reliability and safety of a product [1,2]. Usually, uncertainties can be classified into two distinct types: aleatory and epistemic uncertainties [3–5]. Aleatory uncertainty describes the inherent variation associated with a physical system or environment, which is often dealt with probability theory [6–9]. Epistemic uncertainty refers to the lack of information or data in some phases of the modeling process, which, therefore, can be reduced with the collection of more information. The probability theory has been traditionally used to model epistemic uncertainty, generally by picking some familiar probability distribution and its associated parameters to represent one's belief in the likelihood of possible values. However, for some distributions (e.g. normal or weibull), even small epistemic uncertainty in probability distribution parameters can cause large changes in the tails of the distributions, which may result in unnegligible influence on the reliability analysis results for practical engineering problems [10].

Evidence theory was proposed and developed by Dempster and Shafer [11,12], which provides a promising supplement to probability theory for representation of epistemic uncertainty [13]. First, evidence theory employs a much more flexible framework with respect to the body of evidence and its measures. For example, when information is enough to construct parameter probability distributions, evidence theory can provide an equivalent description to probability theory model. Second, evidence theory can deal directly with situations in which both aleatory and epistemic uncertainties exist. This capability is important because the available data in many engineering problems commonly contain both interval-valued information (epistemic uncertainty) and probability distributions (aleatory uncertainty). Third, evidence theory does not require the assumption of input probability distributions when there is a lack of information.

Due to the above advantages, evidence theory has recently been applied in structural reliability analysis and design. Some exploratory work in this area has been reported, which can be classified into several main categories:

(i) *Comparison between evidence theory and the other uncertainty analysis models.* Several methods for obtaining the evidence theory and probability boxes structures were introduced in [14], which shows that these two structures can be interconvertible. Probability theory, evidence theory, possibility theory and interval analysis were explored and compared in uncertainty representation and propagation with some benchmark problems [15]. Evidence theory and Bayesian theory were compared in uncertainty modeling and decision making, which indicates that Bayesian probabilities can help make a decision when there is considerable uncertainty [16].

* Corresponding author. Tel.: +86 731 88823325; fax: +86 731 88821748.
E-mail address: jiangc@hnu.edu.cn (C. Jiang).

http://dx.doi.org/10.1016/j.ress.2014.12.011
0951-8320/

(ii) *Reliability analysis*. An evidence theory model considering dependence between parameters was formulated for the structural reliability analysis [17]. A structural reliability analysis method using evidence theory was developed by introducing a non-probabilistic reliability index approach [18]. By integrating the moment concept and finite element method, a static and dynamic response analysis approach was formulated for structures with epistemic uncertainty [19]. A sampling-based approach [20] and a semi-analytic approach [21] were developed for sensitivity analysis of the uncertainty propagation problems using evidence theory.

(iii) *Reliability based design optimization*. A design optimization method was developed to handle the mixed epistemic and random uncertainties, in which the vicinity of the optimal point and the active constraints are quickly identified and hence a high computational efficiency is achieved [22]. An evidence-theory-based multidisciplinary design optimization method was proposed for structures with epistemic uncertainty through a sequential approximate strategy [23]. Based on combined probability and evidence theory, a reliability-based multidisciplinary design optimization approach was proposed for the mixed aleatory and epistemic uncertainties [24].

Though some important progresses were achieved above, evidence theory was barely used in practical engineering applications. One main reason is the high computational cost [25]. In evidence-theory-based reliability analysis, the uncertainty is propagated through a discrete probability assignment due to limited information, which is generally described by a series of discontinuous sets rather than an explicit continuous function like the probability density function in probability theory. Thus, time-consuming uncertainty analyses are required among each set for the assessment of its contribution to the reliability, which will inevitably result in expensive computational cost for a multidimensional problem when using evidence theory to conduct the reliability analysis. Aiming at this issue, several numerical methods [25–27] have been proposed to improve the computational efficiency, mainly by introducing the response surface technique. However, the precision of these methods is not usually stable since the response surface is influenced by many factors such as the selection of sampling techniques and approximation model types, and so on. As discussed above, actually a close relationship exists between evidence theory and probability theory, and that is why in many cases evidence theory is also called “imprecise probability”. It then seems natural and also reasonable that some important concepts or well-established techniques in traditional probabilistic reliability analysis could be introduced into the evidence-theory-based reliability analysis, based on which a series of effective reliability methods might be developed.

In this paper, the first and second order approximate reliability methods are proposed for evidence theory, which can significantly improve the computational efficiency of evidence-theory-based reliability analysis. The remainder of this paper is organized as follows. The conventional reliability analysis using evidence theory is introduced in Section 2. The first order approximate reliability method (FARM) and second order approximate reliability method (SARM) are formulated in Section 3. Three numerical examples are investigated in Section 4. Finally conclusions are summarized in Section 5.

2. Conventional reliability analysis using evidence theory

Consider the following reliability analysis problem:

$$g(\mathbf{X}) = g_0 \tag{1}$$

where $\mathbf{X}$ is a vector of n independent uncertain input parameters and they are modeled by the evidence variables in this paper; $g(\mathbf{X})$ is the limit-state function which is usually used to describe the safety or failure state of a structure; g_0 denotes an allowable value of the limit-state function. The safety region G for this problem is defined as:

$$G = \{\mathbf{X} | g(\mathbf{X}) \geq g_0\} \tag{2}$$

The conventional reliability analysis using evidence theory is illustrated with the above simple example, which includes two main steps: the construction of joint basic probability assignment and the computation of reliability interval.

2.1. Construction of joint basic probability assignment

Evidence-theory-based reliability analysis starts by defining a frame of discernment (FD) that is a set of mutually exclusive elementary subsets for each evidence variable X, which is similar to the sample space in probability theory. The FDs for all evidence variables in a problem form the uncertainty domain. In this paper, The FD is also denoted as X. All the possible values of the FD will form a power set $\Omega(X)$.

After defining the FD, the basic probability assignment (BPA) that represents the degree of belief is assigned to each subset of the FD power set based on the statistical data or the expert experience. The BPA is assigned through a mapping function: $\Omega(X) \rightarrow [0, 1]$ which should satisfy the following three axioms:

$$m(A) \geq 0 \quad \text{for any } A \in \Omega(X) \tag{3}$$

$$m(\varnothing) = 0 \tag{4}$$

$$\sum_{A \in \Omega(X)} m(A) = 1 \tag{5}$$

where $m(A)$ refers to the degree of belief that is assigned to the subset A. In this paper, we assume that the subsets A are all closed intervals. Each set $A \in \Omega(X)$ satisfying $m(A) > 0$ is called the focal element. Sometimes the information available for a parameter may come from different sources, thus, the evidence should be aggregated by rules of combination [12,28,29].

Similar to the joint probability density function in probability theory, the joint basic probability assignment should be constructed in evidence theory when multiple uncertain variables are involved. Due to the independence among the parameters, the joint basic probability assignment m can be obtained for an n-dimensional problem as below:

$$m(A) = \begin{cases} \prod_{i=1}^{n} m_i(A_i) & \text{when } A_i \in \Omega(X_i),\ i = 1, 2, \ldots, n \\ 0 & \text{otherwise} \end{cases} \tag{6}$$

where A_i and $\Omega(X_i)$ are the focal element and FD power set of the parameter X_i, respectively, and A is the focal element of the Cartesian Product Θ, which can be defined as follows:

$$\begin{aligned} \Theta &= \Omega(X_1) \times \Omega(X_2) \cdots \times \Omega(X_j) \cdots \times \Omega(X_n) \\ &= \{A = [A_1, A_2, \ldots, A_i, \ldots, A_n], A_i \in \Omega(X_i), \quad i = 1, 2, \ldots, n\}, \quad 1 \leq j \leq n \end{aligned} \tag{7}$$

2.2. Computation of reliability interval

It should be pointed out that evidence theory employs an interval composed of the belief measure (Bel) and the plausibility measure (Pl) to characterize uncertainty of the structural response, rather than a single measure in probability theory.

Based on the obtained joint BPA and the given safety region, the reliability interval $[Bel(G), Pl(G)]$ of the safety event $X \in G$ for the above example can be calculated as below:

$$Bel(G) = \sum_{A \subseteq G} m(A) \tag{8}$$

$$Pl(G) = \sum_{A \cap G \neq \phi} m(A) \tag{9}$$

The belief measure $Bel(G)$ and plausibility measure $Pl(G)$ can be regarded as the lower and upper bounds of the probability measure, which together bracket the true probabilistic reliability p_r [22]:

$$Bel(G) \le p_r \le Pl(G) \tag{10}$$

To calculate $Bel(G)$ and $Pl(G)$, the extreme values $[g_{\min}, g_{\max}]$ of the limit-state function g over each focal element A need to be computed:

$$[g_{\min}, g_{\max}] = \left[\min_{\mathbf{X} \in A} g(\mathbf{X}), \max_{\mathbf{X} \in A} g(\mathbf{X})\right] \tag{11}$$

In addition to the optimization methods, the vertex method [30] is usually adopted to compute $g_{\min}$ and $g_{\max}$ for the computational efficiency. After obtaining the extreme values $[g_{\min}, g_{\max}]$ for each focal element, the BPAs are assigned to the Bel and Pl measures appropriately according to Eqs. (8) and (9). For a focal element with $g_{\min}$ and $g_{\max}$ both larger than the allowable threshold g_0, its corresponding BPA contributes to the calculation of both Bel and Pl. For a focal element with only $g_{\max}$ larger than g_0, its BPA contributes to only Pl. Otherwise, the focal element contributes to neither Bel nor Pl.

3. Efficient reliability analysis methods

In traditional probability-theory-based reliability analysis, the first order reliability method (FORM) [31,32] and second order reliability method (SORM) [33,34] have been proposed, which make the computation of structural reliability very efficient and therefore significantly extend the practical application of probabilistic reliability theory. As shown in Fig. 1(a), FORM and SORM utilize the first and second order Taylor series to approximate the limit-state function at the most probable point (MPP), which has the largest joint probability density among all the points on the limit-state surface and hence contributes most to the calculation of the reliability. Since the approximation is performed at the most important MPP, generally an acceptable accuracy is provided when using FORM and SORM to conduct reliability analysis for practical engineering problems [35].

In evidence-theory-based reliability analysis, a similar important 'region' like the MPP also exists. However, due to the discreteness of BPA, this region is not a point but a focal element, which is generally a multidimensional box in the parameter space. It is defined as the most probable focal element (MPFE) in our previous work [36]. As shown in Fig. 1(b), the MPFE is a focal element intersecting with the limit-state surface, $g(\mathbf{X}) = 0$, and simultaneously has the maximum BPA. Just like the MPP in probabilistic reliability analysis, here the MPFE should have a maximum contribution to the evidence reliability. Thus if we conduct the reliability analysis through approximating the limit-state function around the MPFE, some reliability analysis methods with high efficiency may be developed. Also, by using different types of approximations for the limit-state function, some different reliability analysis methods could be developed. In this paper, just like FORM and SORM, we employ the linear and quadratic Taylor series to approximate the limit-state function around the MPFE, respectively, and whereby propose two efficient evidence-theory-based reliability analysis methods. They are called the first order approximate reliability method (FARM) and the second order approximate reliability method (SARM), respectively.

3.1. First order approximate reliability method (FARM)

By using FARM, the MPFE is first searched using a uniformity approach. Then, the limit-state function is approximated around the MPFE using a linear Taylor series, based on which the reliability interval [Bel, Pl] is calculated efficiently.

3.1.1. Search of the MPFE

As introduced above, the MPFE is the focal element which intersects with the limit-state surface and furthermore possesses the maximum BPA. Generally, it is difficult to search this MPFE directly, since a large number of focal elements will be involved for a multidimensional problem. To improve the efficiency, a uniformity approach [36] is suggested to quickly locate the MPFE. As mentioned previously, the focal elements of each evidence variable in this paper are considered as closed intervals. For most engineering problems, the uncertainty of an imprecise parameter generally behaves as a small perturbation around its nominal value. That is to say, the FD of a practical evidence variable is generally a narrow interval. Therefore, the focal elements, namely the subintervals of the FDs, are even narrower. Thus for convenience of analysis, we can assume a uniform distribution over the interval of each focal element, which generally will not bring large errors.

As shown in Fig. 2, an evidence variable X is transformed to a random variable Y with the following density function f_Y through the uniformity approach:

$$f_Y(y) = \sum_{j=1}^{C(X)} \delta_j(y) m(A_j)/(R_j - L_j) \tag{12}$$

where (i) y is one value contained in the FD of X, (ii) $C(X)$ is the number of focal elements of X, (iii) $A_j = [L_j, R_j], j = 1, 2, \ldots, C(X)$ are the focal elements, with L_j and R_j as the corresponding lower and upper bounds, (iv) $\delta_j(y) = 1$ if $y \in A_j$ and 0 otherwise. Through this treatment, the original limit-state function $g(\mathbf{X})$ with epistemic uncertainty is transformed to $g(\mathbf{Y})$ with only random uncertainty. The reliability analysis problem for $g(\mathbf{Y})$ can be solved by the efficient FORM [31,32] in probability theory. First, the non-normal random variables $\mathbf{Y}$ should be transformed to standard normal variables $\mathbf{U}$:

$$u_i = \phi^{-1}\{F_{Y_i}(y_i)\}, i = 1, 2, \ldots, n \tag{13}$$

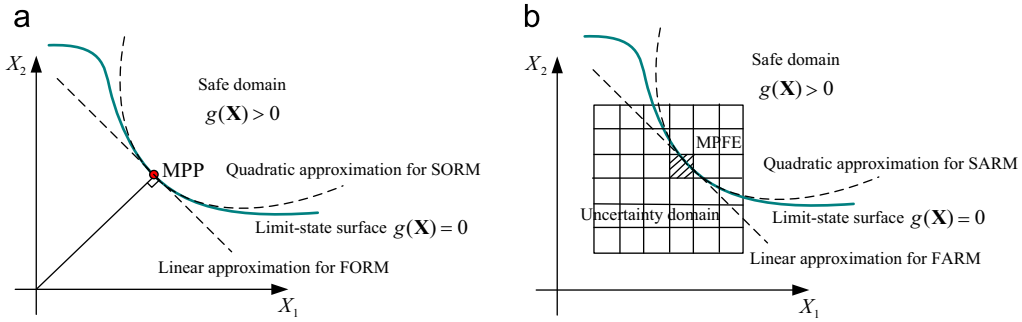

Fig. 1. Comparison of MPP in FORM & SORM (a) and MPFE in FARM & SARM (b).

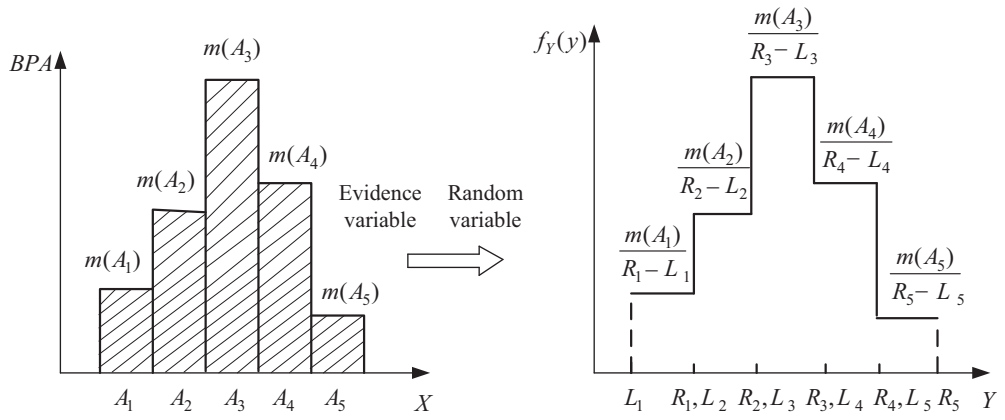

Fig. 2. Transformation from an evidence variable to a random variable using the uniformity approach.

where F_{Y_i} is the cumulative distribution function (CDF) of Y_i, and ϕ^{-1} is the inverse CDF of the standard normal distribution. Through this treatment, $g(\mathbf{Y})$ is transformed to a function $G(\mathbf{U})$ in the standard normal space. The MPP for $G(\mathbf{U})$ can be identified through solving the following optimization problem:

$$\begin{cases} \min\limits_{\mathbf{U}} \|\mathbf{U}\| \\ \text{s.t. } G(\mathbf{U}) = 0 \end{cases} \tag{14}$$

The improved HL-RF (*i*HL-RF) algorithm [37,38] is adopted to solve the above optimization problem and a final $\mathbf{U}^*$ is obtained. After transforming $\mathbf{U}^*$ into the original space, the MPP $\mathbf{X}^*$ for the original reliability problem is obtained, which locates on the limit-state surface and has the largest joint probability density. As mentioned before, the uniformity process that transforms the evidence variables to the random variables generally does not bring about large deviations, since for most practical problems the intervals of the focal elements for a parameter are very narrow. Thus we can be sure that the neighborhood of the obtained MPP should have a maximum contribution to the reliability of the original problem with evidence variables. That is to say, the required MPFE is just the focal element which contains the MPP $\mathbf{X}^*$.

3.1.2. Linear approximation of the limit-state function

The limit-state function $g(\mathbf{X})$ is approximated by the first order Taylor series at the MPP $\mathbf{X}^*$:

$$g(\mathbf{X}) \approx g'(\mathbf{X}) = g(\mathbf{X}^*) + (\mathbf{X} - \mathbf{X}^*)^T \nabla g(\mathbf{X}^*) \tag{15}$$

where $\nabla g(\mathbf{X}^*)$ denotes the gradient vector of the limit-state function at $\mathbf{X}^*$ and it can be computed by the difference method for an implicit problem. With this linear approximate function, the reliability interval [Bel, Pl] can be computed efficiently.

Instead of the original limit-state function $g(\mathbf{X})$, the minimum and maximum values of the approximate limit-state function $g'(\mathbf{X})$ over each focal element should be calculated, respectively:

$$\begin{aligned} &\min_{\mathbf{X} \in A} / \max g'(\mathbf{X}) = g(\mathbf{X}^*) + (\mathbf{X} - \mathbf{X}^*)^T \nabla g(\mathbf{X}^*) \\ &\text{s.t.} \quad A = \left\{ \mathbf{X}^{L_A} \le \mathbf{X} \le \mathbf{X}^{R_A} \right\} \end{aligned} \tag{16}$$

where $\mathbf{X}^{L_A}$ and $\mathbf{X}^{R_A}$ are the lower and upper bound vectors of the focal element A. Since $g'(\mathbf{X})$ is a linear function of $\mathbf{X}$, the extreme values of $g'(\mathbf{X})$ over each focal element can be conveniently obtained according to the signs of $\nabla g(\mathbf{X}^*)$. To illustrate this, one focal element A in a two dimensional problem is considered as shown in Fig. 3. It can be seen that the limit-state function gradients at MPP $\mathbf{X}^*$ $\partial g(\mathbf{X}^*)/\partial X_1 < 0$ and $\partial g(\mathbf{X}^*)/\partial X_2 > 0$, which means that $g'(\mathbf{X})$ is monotonically decreasing along the axis X_1 but

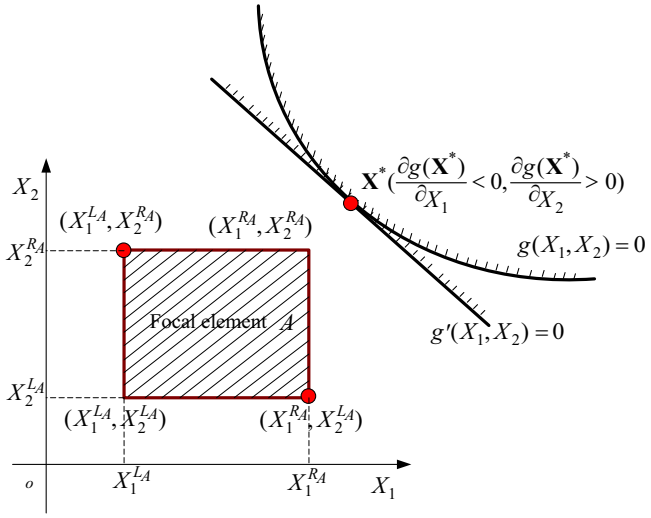

Fig. 3. Extreme analysis using signs of $\nabla g(\mathbf{X}^*)$.

increasing along the axis X_2. Therefore, the maximum function value $g'_{\max}$ and minimum function value $g'_{\min}$ over this focal element are obtained on the points $(X_1^{L_A}, X_2^{R_A})$ and $(X_1^{R_A}, X_2^{L_A})$, respectively. After obtaining the extreme values over each focal element, the Bel and Pl measures can be quickly obtained by assigning the BPAs according to Eqs. (8) and (9).

3.2. Second order approximate reliability method (SARM)

To improve the approximation precision, especially for problems with stronger nonlinearity, a higher order approximate method named SARM is developed. SARM also consists of two steps. In the first step, the MPFE is searched, which is the same as that in FARM. In the second step, the limit-state function is approximated using a quadratic Taylor series, based on which the reliability interval is calculated.

3.2.1. Quadratic approximation of the limit-state function

By solving Eq. (14) and transforming the obtained $\mathbf{U}^*$ into the original space, the MPP $\mathbf{X}^*$ for the original limit-state function $g(\mathbf{X})$ is obtained. Subsequently, $g(\mathbf{X})$ is expanded into the Taylor series at $\mathbf{X}^*$ up to the second order:

$$g(\mathbf{X}) \approx g''(\mathbf{X}) = g(\mathbf{X}^*) + (\mathbf{X} - \mathbf{X}^*)^T \nabla g(\mathbf{X}^*) + \frac{1}{2}(\mathbf{X} - \mathbf{X}^*)^T \nabla^2 g(\mathbf{X}^*)(\mathbf{X} - \mathbf{X}^*) \tag{17}$$

where $\nabla^2 g(\mathbf{X}^*)$ denotes the Hessian matrix of the limit-state function at $\mathbf{X}^*$, which can also be computed using the difference method for an implicit problem. Here, $\nabla^2 g(\mathbf{X}^*)$ is assumed to be a positive definite matrix, which generally holds for practical engineering problems.

To compute the reliability interval, the extreme values of the approximate limit-state function $g''(\mathbf{X})$ over each focal element A should be calculated:

$$\min_{\mathbf{X}\in A} / \max_{\mathbf{X}\in A} g''(\mathbf{X}) = g(\mathbf{X}^*) + (\mathbf{X}-\mathbf{X}^*)^T \nabla g(\mathbf{X}^*) + \tfrac{1}{2}(\mathbf{X}-\mathbf{X}^*)^T \nabla^2 g(\mathbf{X}^*)(\mathbf{X}-\mathbf{X}^*)$$

$$\text{s.t.} \quad A = \left\{ \mathbf{X}^{L_A} \le \mathbf{X} \le \mathbf{X}^{R_A} \right\} \tag{18}$$

Eq. (18) is a quadratic programming problem, which can be solved by using some well-established quadratic programming algorithms [39]. However, it should be pointed out that these conventional algorithms will generally output the local optimums related to the initial points, which therefore is likely to cause large errors of the reliability analysis results for those problems with multiple local optimums. Actually, Eq. (18) belongs to this type of problem. Considering the optimization problem in Eq. (18) has only simple bounding constraints, therefore, we actually could find the global extreme values through the following suggested approach, and hence ensure a higher reliability analysis accuracy.

According to the characteristics of quadratic function, $g''(\mathbf{X})$ will have a global extreme point $\mathbf{X}^e$ over the infinite parameter space under the condition that its Hessian matrix is a positive definite matrix. $\mathbf{X}^e$ can be obtained through the following necessity condition:

$$\nabla g''(\mathbf{X}) = \nabla g(\mathbf{X}^*) + (\mathbf{X}-\mathbf{X}^*)^T \nabla^2 g(\mathbf{X}^*) = 0 \tag{19}$$

Therefore, we have:

$$\mathbf{X}^e = \mathbf{X}^* - \nabla g(\mathbf{X}^*)\left[\nabla^2 g(\mathbf{X}^*)\right]^{-1} \tag{20}$$

When the bounding constraints are applied as in Eq. (18), $g''(\mathbf{X})$ will then have two extreme values, namely the maximum and minimum ones, over each focal element. And they can be obtained through functional evaluations at only a small number of points of $\mathbf{X}$ over each focal element, instead of using the complex optimization solution. Here, we will compute the extreme values according to different cases:

(I) As introduced previously, the FDs described by the variable bounds together form the uncertainty domain, $\mathbf{X}^I = \left\{ \mathbf{X}^L \le \mathbf{X} \le \mathbf{X}^R \right\}$. When $\mathbf{X}^e$ is located inside the uncertainty domain as shown in Fig. 4(a), it must fall in one focal element, e.g. B. Then we will have a set of $\mathbf{X}$ points composed by $\mathbf{X}^e$ and the 2^n vertex points of B. Within the focal element B, $g''(\mathbf{X})$ is not monotonous. But according to the characteristics of quadratic function its two extreme values will be reached at two certain points among the above created set. Thus we only need to compute the values of $g''(\mathbf{X})$ for the points in the set and select the largest and smallest ones as the required two extreme values. While for the other focal elements $g''(\mathbf{X})$ is monotonous and the extreme values can be obtained only on the vertex points.

(II) When $\mathbf{X}^e$ is located outside the uncertainty domain as shown in Fig. 4(b), $g''(\mathbf{X})$ will be monotonous over all the uncertainty domain and therefore its extreme values over each focal element can be obtained directly by comparing functional values on the corresponding vertex points.

Since no assumption is made during the above process, the extreme values $[g''_{\min}, g''_{\max}]$ of $g''(\mathbf{X})$ over each focal element can be obtained accurately and robustly. Furthermore, instead of the local extreme function values, the global values are obtained using the present technique, which, therefore, can help improve the accuracy of SARM. Afterwards, the Bel and Pl measures for SARM will be efficiently calculated using Eqs. (8) and (9).

4. Numerical examples

4.1. Numerical example 1

Consider the following limit-state function:

$$g(X_1, X_2) = \kappa(X_1 - X_2)^2 - X_1 - X_2 - \alpha \tag{21}$$

where the FDs of evidence variables X_1 and X_2 are both $[-2, 2]$; κ reflects the nonlinearity of the limit-state function; α denotes the threshold of the limit-state function. The BPA structure that each variable contains 10 subintervals is considered and the detailed information is given in Table 1.

In order to give a better assessment about the computational accuracy and cost of the proposed FARM and SARM, the direct reliability analysis based on the original limit-state function, as introduced in Section 2, is adopted to provide the reference results, and it is denoted as the conventional method. Also, our recently proposed method [18], termed as non-probabilistic index based reliability method (NIRM), is adopted to provide the results for comparison. Through adjusting the threshold α, a set of different limit-state functions are obtained, while κ is fixed at 0.03.

The computational cost is obtained for four different α as shown in Fig. 5. It can be found that the proposed FARM and SARM are much more efficient than the conventional method, requiring almost only one tenth of the function evaluations of the conventional method for all α values. For example, the function evaluation number of the conventional method is 400 at $\alpha = -0.63$, which, however, is only 31 and 41 for FARM and SARM, respectively. Due to the computation of Hessian matrix,

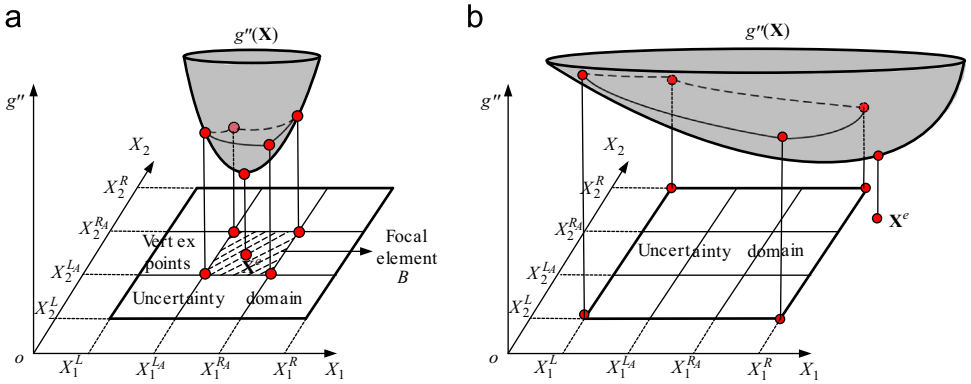

Fig. 4. Two different location cases of $\mathbf{X}^e$ (a) Inside the uncertainty domain and (b) Outside the uncertainty domain.

SARM needs 10 more function evaluations than the FARM. On the other hand, though NIRM has saved much computational cost than the conventional method, its computational efficiency is much less than FARM and SARM. For example, the function evaluation number of NIRM is 300 at $\alpha=-0.63$, almost eight times of the function evaluations of FARM and SARM.

The reliability analysis results are obtained for different α values as shown in Table 2. It can be found that when α varies from -0.05 to -4.11, SARM and NIRM provides exactly the same results as the reference ones for all the cases. For SARM, it is because that the limit-state functions are quadratic and hence the exact results can be obtained using a second order Taylor series approximation. For NIRM, it is because that the limit-state functions are simple and symmetrical about the line $X_1=X_2$ and therefore the exact non-probabilistic indexes are easily obtained, which guarantees the accuracy of the reliability results. FARM performs not so accurately as SARM and NIRM and in some cases there is a slight deviation between its results and the reference ones. It is because that the approximation errors are introduced when using the linear Taylor series to replace the nonlinear limit-state function. However, its computational errors are still acceptable for practical applications. As shown in Table 2, for many cases, FARM provides even exactly the same results as the reference ones. For the other cases, the largest deviation for the belief and plausibility measures of FARM is only 2.5% and 0.7%, respectively, which occurs at the same $\alpha=-0.63$.

Finally, we would analyze the influence of the limit-state function nonlinearity on the precision of FARM and SARM. In this problem, κ changes from 0.03 to 2.1 while α is fixed at 0.2. The results are shown in Table 3. It can be found that FARM provides exactly the same Bel and Pl results under all cases, since a linear approximation is used and hence the nonlinearity of the limit-state function cannot be reflected in FARM. When the nonlinearity is small, the Bel and Pl results from FARM are very close to the reference ones. For example, at $\kappa=0.07$, the deviation of the belief measure for FARM is only 3.13% and that of the plausibility measure is only 1.72%. With the increase of the nonlinearity degree, the Bel and Pl results from FARM gradually behave a larger deviation from the reference ones. In SARM, the nonlinearity is reflected by the second order Taylor series, thus, it provides very good reliability analysis results for all cases. Actually, for this problem, the results are exactly the same as the reference ones. Thus, from the numerical example, it can be found that for problems with relatively weak nonlinearity, FARM can be used to obtain a sufficiently precise result, while for problems with relatively strong nonlinearity SARM is recommended for use. On the other hand, though SARM is generally more accurate than FARM, it seems a little more complex and time-consuming than the latter.

Table 1
The 10-subinterval BPA structure for variables X_1 and X_2.

X_1		X_2	
Subinterval	BPA	Subinterval	BPA
[−2.0, −1.6]	0.02	[−2.0, −1.6]	0.02
[−1.6, −1.2]	0.06	[−1.6, −1.2]	0.06
[−1.2, −0.8]	0.10	[−1.2, −0.8]	0.10
[−0.8, −0.4]	0.14	[−0.8, −0.4]	0.14
[−0.4,0]	0.18	[−0.4,0]	0.18
[0,0.4]	0.18	[0,0.4]	0.18
[0.4,0.8]	0.14	[0.4,0.8]	0.14
[0.8,1.2]	0.10	[0.8,1.2]	0.10
[1.2,1.6]	0.06	[1.2,1.6]	0.06
[1.6,2.0]	0.02	[1.6,2.0]	0.02

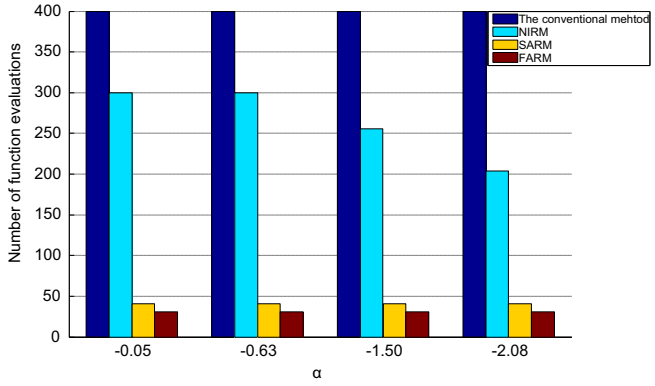

Fig. 5. Comparison of computational cost among FARM, SARM, NIRM and the conventional method.

4.2. Numerical example 2

A crank-slider mechanism as shown in Fig. 6 is investigated, which is modified from [40].The inner diameter d_1 and outer diameter d_2 of the coupler are 10 mm and 20 mm, respectively. The coefficient of friction u between the ground and the slider is

Table 3
Comparison of precision between FARM and SARM when under different values of κ.

κ	Reference results	FARM	Deviations	SARM	Deviations
	[Bel, Pl]	[Bel, Pl]		[Bel, Pl]	
0.03	[0.31, 0.57]	[0.31, 0.57]	[0%, 0%]	[0.31, 0.57]	[0%, 0%]
0.07	[0.32, 0.58]	[0.31, 0.57]	[3.13%, 1.72%]	[0.32, 0.58]	[0%, 0%]
0.1	[0.36, 0.61]	[0.31, 0.57]	[13.89%, 6.56%]	[0.36, 0.61]	[0%, 0%]
0.5	[0.54, 0.75]	[0.31, 0.57]	[42.59%, 24.00%]	[0.54, 0.75]	[0%, 0%]
0.9	[0.54, 0.78]	[0.31, 0.57]	[42.59%, 26.92%]	[0.54, 0.78]	[0%, 0%]
1.3	[0.57, 0.82]	[0.31, 0.57]	[45.61%, 31.70%]	[0.57, 0.82]	[0%, 0%]
1.7	[0.61, 0.89]	[0.31, 0.57]	[49.18%, 35.96%]	[0.61, 0.89]	[0%, 0%]
2.1	[0.61, 0.89]	[0.31, 0.57]	[49.18%, 35.96%]	[0.61, 0.89]	[0%, 0%]

Table 2
Comparison of precision among FARM, SARM, NIRM and the conventional method under different α.

α	Reference results [Bel, Pl]	FARM [Bel, Pl]	Deviations	SARM [Bel, Pl]	Deviations	NIRM [Bel, Pl]	Deviations
−0.05	[0.435, 0.691]	[0.434, 0.691]	[0.2%, 0%]	[0.435, 0.691]	[0%, 0%]	[0.435, 0.691]	[0%, 0%]
−0.63	[0.580, 0.804]	[0.566, 0.798]	[2.5%, 0.7%]	[0.580, 0.804]	[0%, 0%]	[0.580, 0.804]	[0%, 0%]
−1.21	[0.798, 0.938]	[0.798, 0.938]	[0%, 0%]	[0.798, 0.938]	[0%, 0%]	[0.798, 0.938]	[0%, 0%]
−1.79	[0.881, 0.972]	[0.881, 0.972]	[0%, 0%]	[0.881, 0.972]	[0%, 0%]	[0.881, 0.972]	[0%, 0%]
−2.37	[0.945, 0.990]	[0.938, 0.990]	[0.8%, 0%]	[0.945, 0.990]	[0%, 0%]	[0.945, 0.990]	[0%, 0%]
−2.95	[0.990, 1]	[0.990, 1]	[0%, 0%]	[0.990, 1]	[0%, 0%]	[0.990, 1]	[0%, 0%]
−3.53	[0.997, 1]	[0.997, 1]	[0%, 0%]	[0.997, 1]	[0%, 0%]	[0.997, 1]	[0%, 0%]
−4.11	[1,1]	[1,1]	[0%, 0%]	[1,1]	[0%, 0%]	[1,1]	[0%, 0%]

0.2. Due to the manufacturing errors and harsh working environment, the length of the crank a, the length of the coupler b and the external force P are treated as evidence variables. Also, different installation positions of the slider are required in various working sites, thus, the offset e is also considered as an evidence variable. The limit-state function is defined as the difference between the material strength and the maximum stress of the coupler:

$$g(a,b,P,e)=S-\frac{4P(b-a)}{\pi\left(\sqrt{(b-a)^2-e^2}-\mu e\right)\left(d_2^2-d_1^2\right)} \tag{22}$$

The FDs for a,b,P,e are determined based on limited historical data and they are [94 mm, 106 mm], [290 mm, 310 mm], [220 kN, 280 kN], [100 mm, 150 mm], respectively. Two different cases that the BPA structure contains 4 and 6 subintervals are investigated in this problem, whose detailed information is given in Tables 4 and 5, respectively.

Fig. 7 gives a comparison of the computational cost among FARM, SARM, NIRM and the conventional method under both BPA structure cases. First, it shows that the conventional method and NIRM require much more function evaluations than the proposed methods under both cases, almost two to three more magnitudes. For example, under the 4-subinterval BPA structure case, the function evaluation number for the conventional method and NIRM at $S=1.98$ is 4096 and 3840, which, however, is only 35 for FARM and 79 for SARM. Though much more time-consuming than FARM and SARM, NIRM is more efficient than the conventional method. Second, it shows that the function evaluation number of the conventional method and NIRM increases sharply when the number of subintervals in the BPA structure increases from 4 to 6. For example, for the same $S=1.98$, the number of the conventional method and NIRM increases from 4096 and 3840 to 20,736 and 16,640, respectively. However, for the proposed methods, the computational cost only shows a tiny fluctuation. Finally, by comparing Figs. 5 and 7, it can be found that the function evaluation number of the conventional method and NIRM increases sharply to a higher order of magnitude with the problem dimension, while that of both FARM and SARM is almost still in the same order of magnitude.

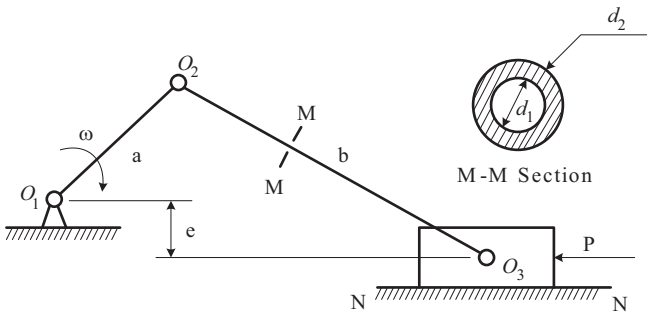

Fig. 6. A crank-slider mechanism [40].

Table 4
The 4-subinterval BPA structure for variables a,b,P and e.

a		b		P		e	
Subinterval	BPA	Subinterval	BPA	Subinterval	BPA	Subinterval	BPA
[94,97]	0.1	[290,295]	0.1	[220,235]	0.1	[100,112.5]	0.1
[97,100]	0.4	[295,300]	0.4	[235,250]	0.4	[112.5,125]	0.4
[100,103]	0.4	[300,305]	0.4	[250,265]	0.4	[125,137.5]	0.4
[103,106]	0.1	[305,310]	0.1	[265,280]	0.1	[137.5,150]	0.1

The reliability analysis results for the 4-subinterval and 6-subinterval BPA structure cases are obtained as shown in Tables 6 and 7, respectively. First, it can be found that with the increase of the number of subintervals for each parameter, the gap between the belief and plausibility results for the same S becomes narrower. In other words, the increasing information of input parameters leads to a lower level of epistemic uncertainty in the response. Second, it can be found that the Bel and Pl results obtained from SARM exactly agree with the reference ones under both cases, which implies its good accuracy for problems with not strong nonlinearity. Thirdly, the Bel and Pl results obtained from NIRM exactly agree with the reference ones at most cases, except at $S=1.86$ and $S=2.10$. The non-probabilistic indexes are not exactly obtained in these cases, which is caused by the fact that using sequential quadratic programming (SQP) to solve the optimization model constructed for the non-probabilistic index [18] seems not to be always stable. Finally, the Bel and Pl results obtained from FARM agree well with the reference ones under both cases, and at many cases they are even exactly the same. The largest deviations of the belief and plausibility measures are only 1.4% and 0.6%, which occurs at $S=1.74$.

4.3. Application to a vehicle crash problem

In recent years, traffic accidents have resulted in thousands of passenger injury and death, among which the frontal impact of vehicle has been the most principal factor. Therefore, much attention has been drawn to the vehicle safety research for the frontal impact. Here, a model of full-width frontal crash as shown in Fig. 8 is investigated. Vehicle safety can be measured by parameters such as the contact forces exerted on the occupants or the resulting accelerations during a vehicle crash [41]. In this application we will carry out a reliability analysis for the mean integration acceleration of the left backseat, which can be calculated as follows:

$$\bar{a}=\max\left[\frac{1}{t_1-t_2}\int_{t_1}^{t_2}a\,dt\right] \tag{23}$$

where t_1 and t_2 are any selected time instances during the testing period which satisfy $t_2-t_1=36$ ms; a is the synthesis acceleration of the left backseat and its unit is the gravitational acceleration, g.

During the vehicle safety design, the front bumper, crash box and front rail are major energy absorbing components which will

Table 5
The 6-subinterval BPA structure for variables a,b,P and e.

a		b		P		e	
Subinterval	BPA	Subinterval	BPA	Subinterval	BPA	Subinterval	BPA
[94,96]	0.1	[290,293.33]	0.1	[220,230]	0.1	[100,108.33]	0.1
[96,98]	0.2	[293.33,296.67]	0.2	[230,240]	0.2	[108.33,116.67]	0.2
[98,100]	0.2	[296.67,300]	0.2	[240,250]	0.2	[116.67,125]	0.2
[100,102]	0.2	[300,303.33]	0.2	[250,260]	0.2	[125,133.33]	0.2
[102,104]	0.2	[303.33,306.67]	0.2	[260,270]	0.2	[133.33,141.67]	0.2
[104,106]	0.1	[306.67,310]	0.1	[270,280]	0.1	[141.67,150]	0.1

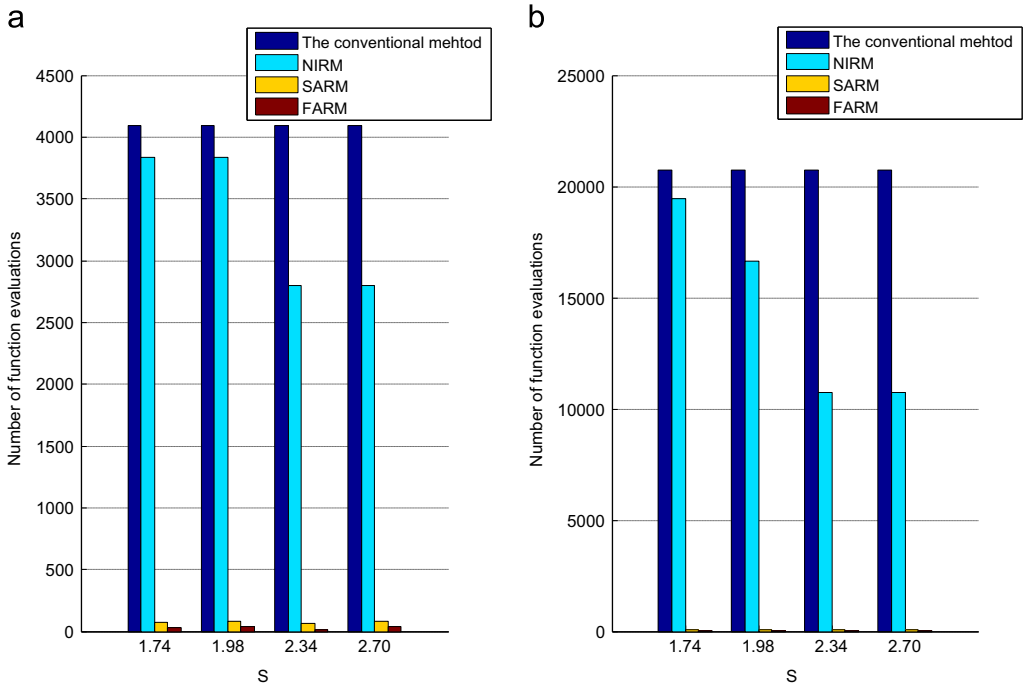

Fig. 7. Comparison of computational cost among FARM, SARM, NIRM and the conventional method under 4-subinterval (Case I) (a) and 6-subinterval (Case II) (b) BPA structures.

Table 6
Comparison of precision among FARM, SARM, NIRM and the conventional method under the 4-subinterval BPA structure.

S	Reference results [Bel, Pl]	FARM [Bel, Pl]	Deviations	SARM [Bel, Pl]	Deviations	NIRM [Bel, Pl]	Deviations
1.74	[0.374, 0.958]	[0.374, 0.958]	[0%, 0%]	[0.374, 0.958]	[0%, 0%]	[0.374, 0.958]	[0%, 0%]
1.86	[0.611, 0.993]	[0.613, 0.993]	[0.3%, 0%]	[0.611, 0.993]	[0%, 0%]	[0.612, 0.993]	[0.2%, 0%]
2.10	[0.898, 1]	[0.900, 1]	[0.2%, 0%]	[0.898, 1]	[0%, 0%]	[0.894, 1]	[0.4%, 0%]
2.22	[0.947, 1]	[0.948, 1]	[0.1%, 0%]	[0.947, 1]	[0%, 0%]	[0.947, 1]	[0%, 0%]
2.34	[0.976, 1]	[0.979, 1]	[0.3%, 0%]	[0.976, 1]	[0%, 0%]	[0.976, 1]	[0%, 0%]
2.46	[0.991, 1]	[0.991, 1]	[0%, 0%]	[0.991, 1]	[0%, 0%]	[0.991, 1]	[0%, 0%]
2.58	[0.998, 1]	[0.998, 1]	[0%, 0%]	[0.998, 1]	[0%, 0%]	[0.998, 1]	[0%, 0%]
2.70	[0.999, 1]	[0.999, 1]	[0%, 0%]	[0.999, 1]	[0%, 0%]	[0.999, 1]	[0%, 0%]

Table 7
Comparison of precision among FARM, SARM, NIRM and the conventional method under the 6-subinterval BPA structure.

S	Reference results [Bel, Pl]	FARM [Bel, Pl]	Deviations	SARM [Bel, Pl]	Deviations	NIRM [Bel, Pl]	Deviations
1.74	[0.508, 0.858]	[0.515, 0.863]	[1.4%, 0.6%]	[0.508, 0.858]	[0%, 0%]	[0.508, 0.858]	[0%, 0%]
1.86	[0.676, 0.950]	[0.683, 0.951]	[1.0%, 0.1%]	[0.676, 0.950]	[0%, 0%]	[0.678, 0.950]	[0.3%, 0%]
2.10	[0.892, 0.998]	[0.896, 0.998]	[0.4%, 0%]	[0.892, 0.998]	[0%, 0%]	[0.905, 0.998]	[1.5%, 0%]
2.22	[0.947, 1]	[0.950, 1]	[0.3%, 0%]	[0.947, 1]	[0%, 0%]	[0.947, 1]	[0%, 0%]
2.34	[0.977, 1]	[0.978, 1]	[0.1%, 0%]	[0.977, 1]	[0%, 0%]	[0.977, 1]	[0%, 0%]
2.46	[0.991, 1]	[0.994, 1]	[0%, 0%]	[0.991, 1]	[0%, 0%]	[0.991, 1]	[0%, 0%]
2.58	[0.997, 1]	[0.998, 1]	[0%, 0%]	[0.997, 1]	[0%, 0%]	[0.997, 1]	[0%, 0%]
2.70	[0.999, 1]	[0.999, 1]	[0%, 0%]	[0.999, 1]	[0%, 0%]	[0.999, 1]	[0%, 0%]

directly affect the vehicle crashworthiness. Due to the manufacturing and measurement errors, here the thicknesses of the front bumper d_1, the crash box inner plate d_2 and outer plate d_3, the front rail inner plate d_4 and outer plate d_5 are treated as evidence variables. Their FDs are [2 mm, 3 mm], [1 mm, 2.5 mm], [1 mm, 2.5 mm], [1.5 mm, 3 mm], [1.5 mm, 3 mm], respectively. The limit-state function is defined as the difference between the allowable mean integration acceleration $\overline{a}'$ of the left backseat and its experimental value $\overline{a}$:

$$g = \overline{a}' - \overline{a}(d_1, d_2, d_3, d_4, d_5) \tag{23}$$

A finite element analysis (FEA) model is created to compute the mean integration acceleration $\overline{a}$ of the left backseat, in which the vehicle impacts the rigid wall with an initial velocity 56.4 km/h at the front. The model has 755 components, 998,220 nodes and 977,742 elements. Due to the high computational cost of this

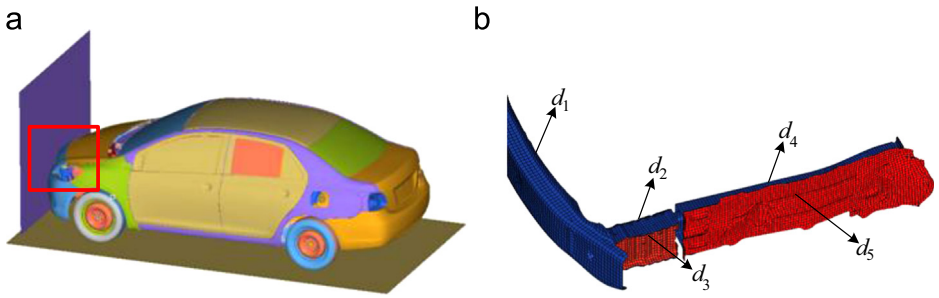

Fig. 8. A vehicle crash problem and its involved uncertain parameters (a) A vehicle frontal collision and (b) The involved uncertain parameters.

Table 8
Reliability results of the vehicle crash problem at $\bar{a}' = 38\ g$.

Methods	Bel	PL	Evaluation number of FEA
FARM	0.7076	1	43
SARM	0.7684	0.9632	113

model, only one case that $\bar{a}' = 38$ g is considered and the reliability analysis results for FARM and SARM are given in Table 8. On one hand, two different reliability intervals $[\mathrm{Bel}, \mathrm{Pl}] = [0.7076, 1]$ and $[\mathrm{Bel}, \mathrm{Pl}] = [0.7684, 0.9632]$ are obtained using FARM and SARM, both of which indicate that the vehicle's acceleration of the left backseat during the frontal impact cannot well satisfy the risk requirement and the passengers have a possibility to be injured. Therefore, a structural modification is needed to improve the vehicle safety. The difference between the reliability results of FARM and SARM is caused by the nonlinearity of the limit-state function. However, the deviation of the belief measure is only 7.91% and that of the plausibility is only 3.82%, which indicates that the nonlinearity of this problem is not too strong and hence both results of FARM and SARM can be accepted. On the other hand, the evaluation number of FEA for FARM is only 43, while that of SARM increases to 113. Since each evaluation of the FEA model takes almost 8 h, the increased computational cost for SARM would be more than 20 days. Therefore, if we pay more attention to the computational cost in this problem, then FARM is preferred. Otherwise, SARM would be preferred for the better accuracy.

5. Conclusions

In this paper, the first order approximate reliability method (FARM) and second order approximate reliability method (SARM) are developed for evidence theory. They approximate the limit-state function using the first and second order Taylor series around the most probable focal element. The efficiency and accuracy of FARM and SARM are studied, compared with the non-probabilistic index based reliability method (NIRM) and the conventional method. Some observations can be obtained from the results of the numerical examples. (1) FARM and SARM are much more efficient than the conventional method and NIRM. As the number of subintervals for the input parameters or the dimension of the problem increases, the efficiency of FARM and SARM becomes even much better. SARM requires a little more computational cost than FARM, which is caused by the calculation of the Hessian matrix. (2) FARM could provide acceptable reliability results for problems with relatively weak nonlinearity. For problems with stronger nonlinearity, SARM is recommended to provide more accurate results. The accuracy of NIRM is supposed to be good for many problems, however, at situations where the non-probabilistic indexes are not exactly obtained, nonnegligible deviations may occur.

Acknowledgements

This work is supported by the Chinese National Science Foundation (11172096), the Chinese National Science Foundation for Excellent Young Scholars (51222502), the program for New Century Excellent Talents in University (NCET-11-0124) and the Excellent Youth Foundation of Hunan Province (14JJ1016).

References

[1] Guo J, Du XP. Sensitivity analysis with mixture of epistemic and aleatory uncertainties. AIAA J 2007;45(9):2337–49.
[2] Gao W, Song CM, Tin-Loi F. Probabilistic interval analysis for structures with uncertainty. Struct Saf 2010;32(3):191–9.
[3] Hoffman FO, Hammonds JS. Propagation of uncertainty in risk assessment: the need to distinguish between uncertainty due to lack of knowledge and uncertainty due to variability. Risk Anal 1994;14(5):707–12.
[4] Ferson S, Ginzburg LR. Different methods are needed to propagate ignorance and variability. Reliab Eng Syst Safe 1996;54:133–44.
[5] Hora SC. Aleatory and epistemic uncertainty in probability elicitation with an example from hazardous waste management. Reliab Eng Syst Safe 1996;54:217–23.
[6] Hasofer AM, Lind NC. Exact and invariant second-moment code format. ASCE J Eng Mech 1974;100:111–21.
[7] Hohenbichler M, Rackwitz R. Non-normal dependent vectors in structural safety. ASCE J Eng Mech 1981;107(6):1227–38.
[8] Sobczyk K, Trcebicki J. Approximate probability distributions for stochastic systems: maximum entropy method. Comput Methods Appl Mech 1999;168(1-4):91–111.
[9] Du XP, Hu Z. First order reliability method with truncated random variables. ASME J Mech Des 2012;134(9):091005.
[10] Oberkampf WL, Helton JC. Investigation of evidence theory for engineering applications. In: 43rd AIAA/ASME/ASCE/AHS/ASC structures, structural dynamics, and materials conference, Denver, Colorado; 2002.
[11] Dempster AP. Upper and lower probabilities induced by a multivalued mapping. Ann Math Stat 1967;38(2):325–39.
[12] Shafer G. A mathematical theory of evidence. NJ: Princeton; 1976.
[13] Oberkampf WL, Helton JC. Mathematical representation of uncertainty. In: 19th AIAA applied aerodynamics conference, Seattle, WA; 2001.
[14] Ferson S, Kreinovich V, Ginzburg L, Myers DS, Sentz K. Constructing probability boxes and Dempster–Shafer structures. Sandia National Laboratories: SAND 2002–4015 report; 2002.
[15] Helton JC, Johnson JD, Oberkampf WL. An exploration of alternative approaches to the representation of uncertainty in model predictions. Reliab Eng Syst Safe 2004;85:39–71.
[16] Soundappan P, Nikolaidis E, Haftka RT, Grandhi R, Canfield R. Comparison of evidence theory and Bayesian theory for uncertainty modeling. Reliab Eng Syst Safe 2004;85:295–311.
[17] Jiang C, Wang B, Li ZR, Han X, Yu DJ. An evidence-theory model considering dependence among parameters and its application in structural reliability analysis. Eng Struct 2013;57:12–22.
[18] Zhang Z, Jiang C, Wang GG, Han X. An efficient reliability analysis method for structures with epistemic uncertainty using evidence theory. In: Proceedings of the ASME 2014 international design engineering technical conference & computers and information in engineering conference, New York, USA; 2014.
[19] Bai YC, Jiang C, Han X, Hu DA. Evidence-theory-based structural static and dynamic response analysis under epistemic uncertainties. Finite Elem Anal Des 2013;68:52–62.

[20] Helton JC, Johnson JD, Oberkampf WL, Sallaberry CJ. Sensitivity analysis in conjunction with evidence theory representations of epistemic uncertainty. Reliab Eng Syst Safe 2006;91:1414–34.
[21] Bae HR, Grandhi RV, Canfield RA. Sensitivity analysis of structural response uncertainty propagation using evidence theory. Struct Multidisc Optim 2006;31:270–9.
[22] Mourelatos Z, Zhou J. A design optimization method using evidence theory. ASME J Mech Des 2006;128:901–8.
[23] Agarwal H, Renaud JE, Preston EL, Padmanabhan D. Uncertainty quantification using evidence theory in multidisciplinary design optimization. Reliab Eng Syst Safe 2004;85:281–94.
[24] Yao W, Chen XQ, Qi QY, Tooren MV. A reliability-based multidisciplinary design optimization procedure based on combined probability and evidence theory. Struct Multidisc Optim 2013;48:339–54.
[25] Bae HR, Grandhi RV, Canfield RA. Epistemic uncertainty quantification techniques including evidence theory for large-scale structures. Comput Struct 2004;82:1101–12.
[26] Bae HR, Grandhi RV, Canfield RA. An approximation approach for uncertainty quantification using evidence theory. Reliab Eng Syst Safe 2004;86:215–25.
[27] Zhang Z, Jiang C, Han X, Hu DA, Yu S. A response surface approach for structural reliability analysis using evidence theory. Adv Eng Software 2014;69:37–45.
[28] Yager RR, Kacprzyk J, Fedrizzi M. Advances in Dempster–Shafer theory of evidence. New York: John Wiley & Sons; 1994.
[29] Sentz K, Ferson S. Combination of evidence in Dempster–Shafer theory. Sandia National Laboratories: SAND2002-0835 report; 2002.
[30] Dong WM, Shah HC. Vertex method for computing functions of fuzzy variable. Fuzzy Sets Syst 1987;24:65–78.
[31] Hasofer AM, Lind NC. Exact and invariant second-moment code format. ASME J Eng Mech Div 1974;100:111–21.
[32] Rackwitz R, Fiessler B. Structural reliability under combined random load sequences. Comput Struct 1978;9(5):489–94.
[33] Breitung KW. Asymptotic approximation for multinormal integrals. ASCE J Eng Mech 1984;110(3):357–66.
[34] Breitung KW. Asymptotic approximations for probability integrals. Berlin: Springer-Verlag; 1994.
[35] Rackwitz R. Reliability analysis—a review and some perspectives. Struct Safe 2001;23:365–95.
[36] Jiang C, Zhang Z, Han X, Liu J. A novel evidence-theory-based reliability analysis method for structures with epistemic uncertainty. Comput Struct 2013;129:1–12.
[37] Zhang Y, Kiureghian A. Two improved algorithms for reliability analysis, Reliability and optimization of structural systems. In: Proceedings of the sixth IFIP WG7.5 working conference on reliability and optimization of structural systems, Assisi, Italy; 1995.
[38] Du XP. Interval reliability analysis. In: International design engineering technical conference and computers and information in engineering conference, Las Vegas, NV; 2007.
[39] Nocedal J, Wright SJ. Numerical optimization. New York: Springer-Verlag; 1999.
[40] Du XP. Unified uncertainty analysis by the first order reliability method. ASME J Mech Des 2008;130(9):1–10 (091401).
[41] Fang H, Rais-Rohani M, Liu Z, Horstemeyer MF. A comparative study of metamodeling methods for multiobjective crashworthiness optimization. Comput Struct 2005;83:2121–36.